Supporting Information

Effect of Solvent Vapour Annealing on Bismuth Triiodide Film for Photovoltaic Applications and its Optoelectronic Properties

Muthu Gomathy M. Pandian,[a,b†] Dhruba B. Khadka,[a†*] Yasuhiro Shirai,[a*] Shodruz Umedov,[a,c] Masatoshi Yanagida,[a] Shanthi Subashchandran,[b] Anastasia Grigorieva,[c] and Kenjiro Miyano[a]

[a]Photovoltaic Materials Group, Center for GREEN Research on Energy and Environmental Materials, National Institute for Materials Science (NIMS), 1-1 Namiki, Tsukuba, Ibaraki 305-0044, Japan.

[b] Crystal Growth Centre, Anna University, Chennai-600025, Tamil Nadu, India.

[c] Faculty of Materials Science and Faculty of Chemistry, Lomonosov Moscow State University, Leninskie gory - 1, bld. 3, Moscow,119991 Russia

Corresponding Author

*KHADKA.B.Dhruba@nims.go.jp

*SHIRAI.Yasuhiro@nims.go.jp

Table and Figures

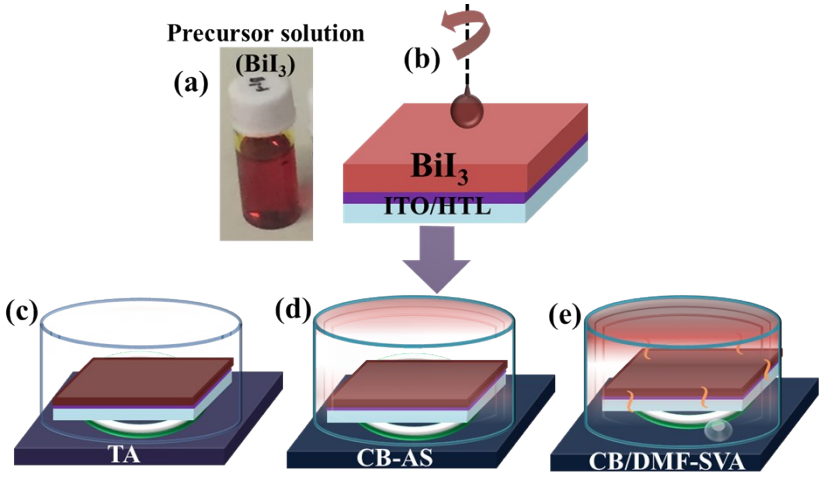

Figure S1. Schematic of the fabrication approach of the BiI_3 thin film. (a) Precursor solution of BiI_3, (b) precursor deposition on the ITO/HTL substrate. The crystallization of BiI_3 thin film by (c) thermal annealing (TA), (d) annealing the antisolvent (chlorobenzene (CB)) dripped film (AS), and (e) annealing under ambient solvent (CB or dimethylformamide (DMF)) vapor (CB or DMF-SVA).

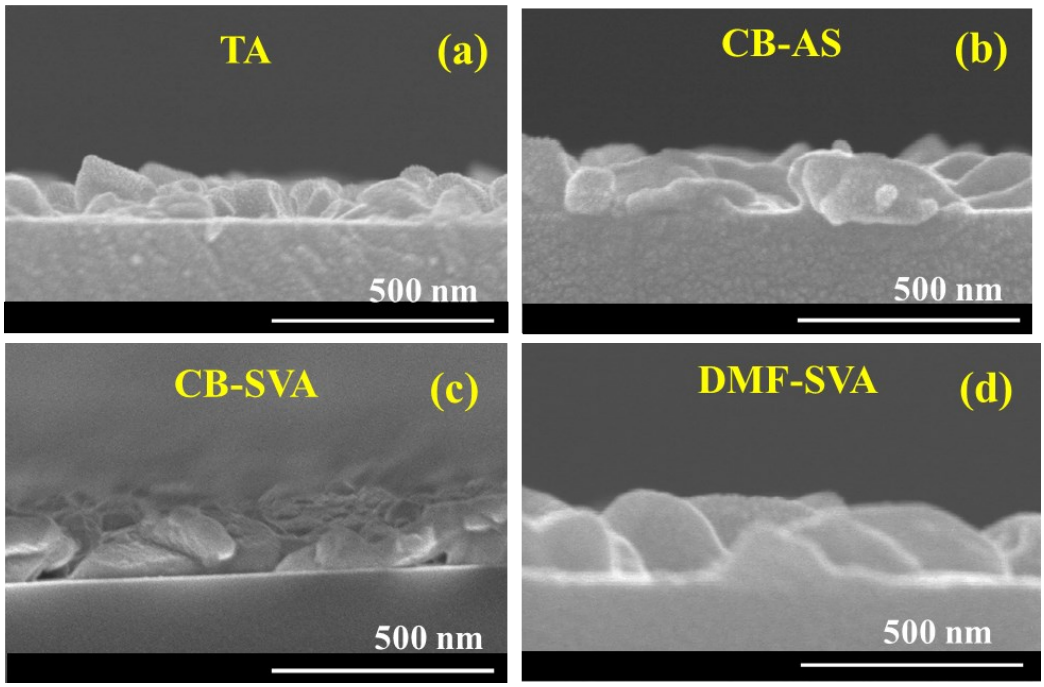

Figure S2. Cross-sectional SEM images of the BiI_3 thin films crystallized via (a) TA, (b) CB-AS, (c) CB-SVA, (d) DMF-SVA.

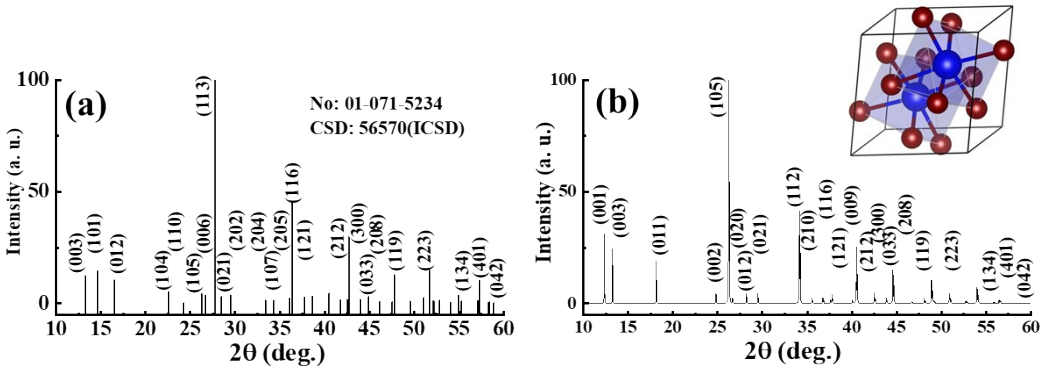

Figure S3. XRD pattern of BiI_3 (tetragonal) (ICSD-56570) as references (Inorganic Crystal Structure Database) and calculated XRD pattern from the VESTA using BiI_3 crystal CIF file.

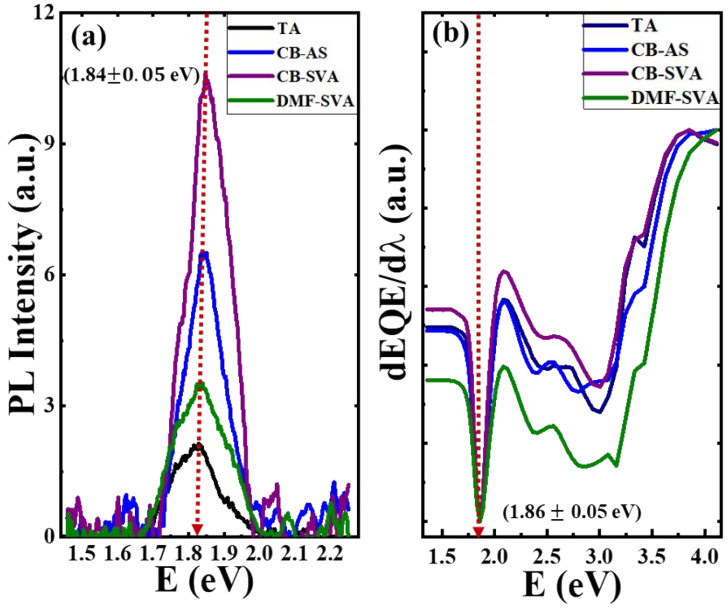

Figure S4. The PL spectra of BiI_3 thin films crystallized under different ambient conditions (a) and (b) bandgap energy (E_g) estimated from the differentiation of EQE spectra (Fig. 3d and Fig. S6b).

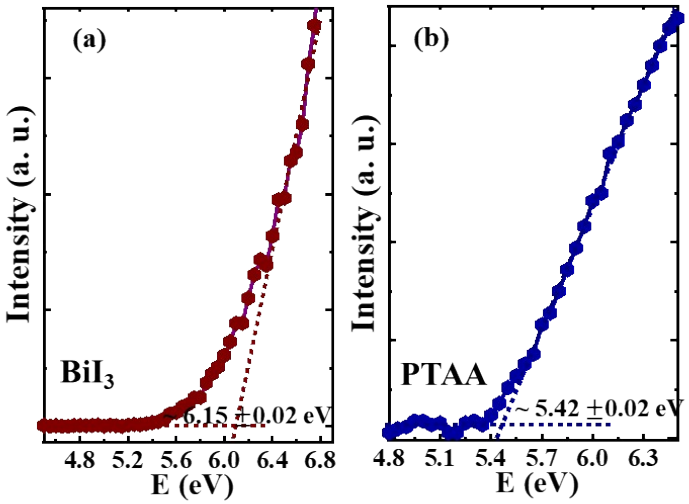

Figure S5. Photoelectron spectra of (a) BiI_3 film and (b) plasma-treated PTAA HTL layer.

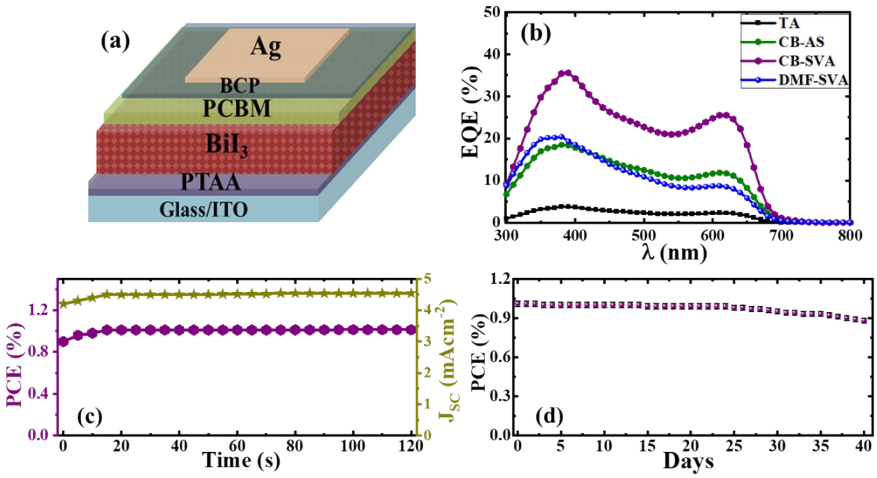

Figure S6. (a) Schematics of the device structure, (b) *EQE* spectra of corresponding devices. (c) Steady-state J_{SC} and PCE of the BiI_3 device prepared by CB-SVA approach at maximum power point tracking (MPPT) under AM 1.5G 100 mW cm^{-2} illumination and (d) stability of the device stored in ambient air conditions.

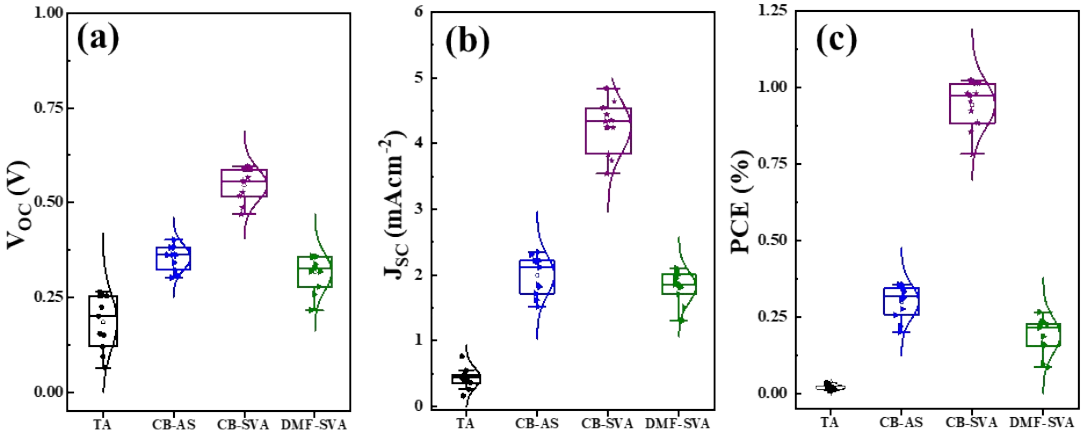

Figure S7. Statistics of device parameters for the BiI_3 based solar cells with BiI_3 thin film fabricated by various methods; TA, CB-AS, CB, or DMF-SVA. Histogram of device parameters: (a) V_{OC}, (b) $J_{SC,}$ and (c) *PCE* (η) of 12 devices fabricated four different batches.

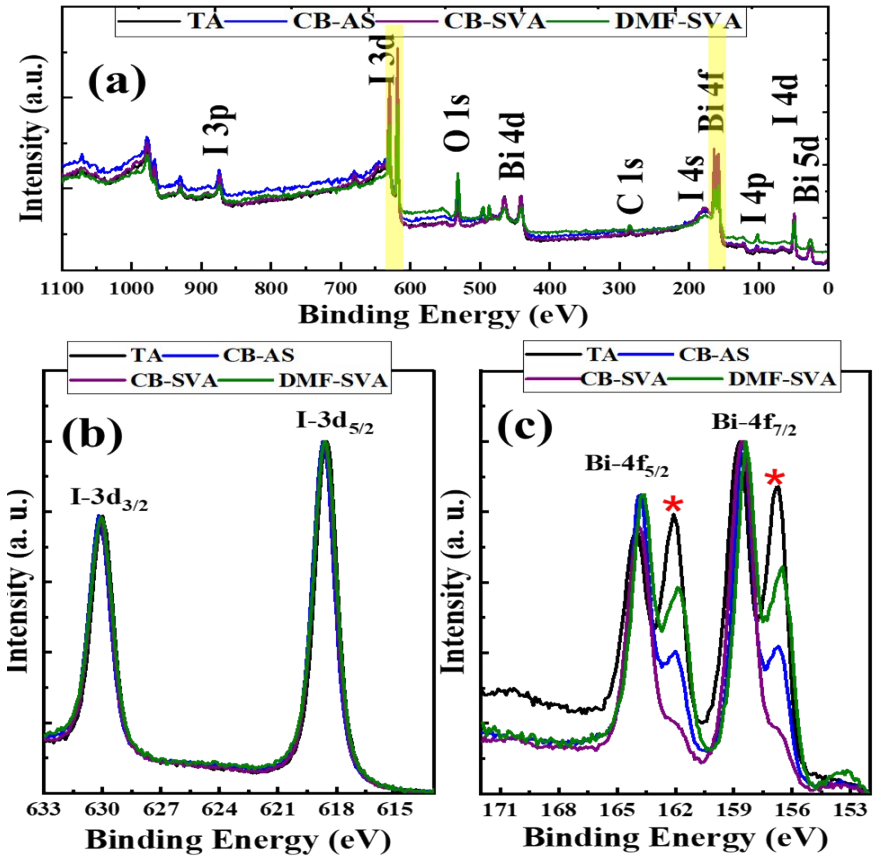

Figure S8. XPS spectra of BiI3 films prepared under different conditions. (a) Survey spectra, (b) The core-level peak for I-3d, and (c) Bi-4f. The two steric symbols in the plot (c) at ~162 eV and 157 eV assigned for metallic Bi. Note that the spectra (b) and (c) are normalized.

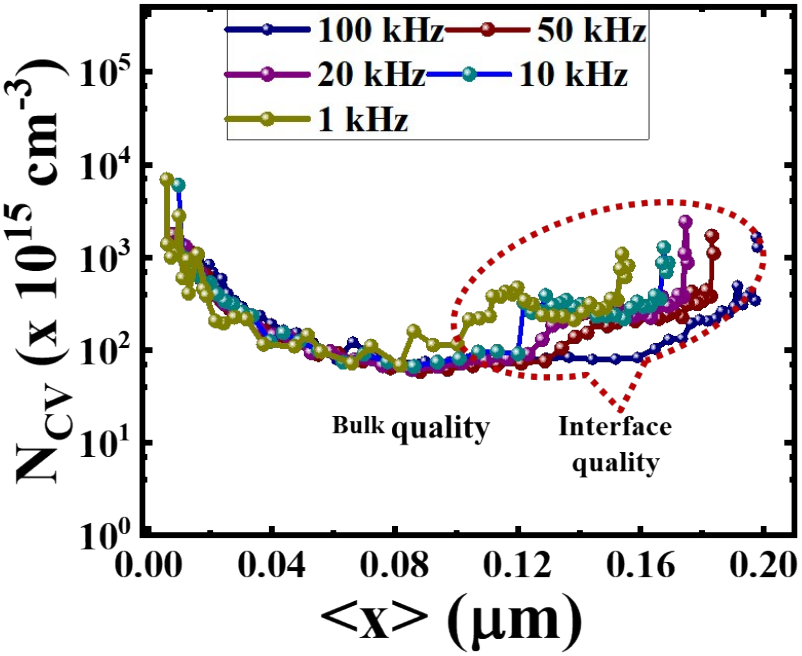

Figure S9. The density (carrier + defect) profile of the BiI_3 device prepared by the CB-SVA approach extracted from capacitance-voltage (*C-V*) curves at different modulated frequencies bias.

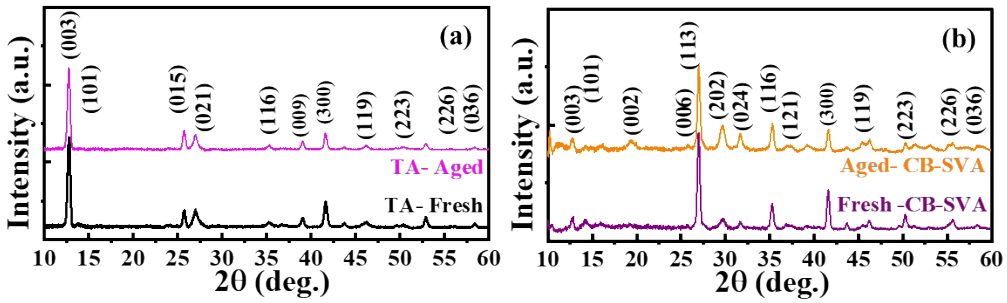

Fig. S10. The XRD patterns of fresh and aged (kept under ambient air for 30 days) BiI_3 (TA (a) and CB-SVA) (b) films.